Journal of Translational Medicine

RESEARCH

Open Access

Homeobox B9 promotes the invasion and metastasis of hepatocellular carcinoma cells via the EZH2–MIR203A–SNAI2 axis

Dandan Zhang[1,2,3,4†], Yumin Qiu[1,2,3,4†], Wenming Zhang[1,2,3,4], Dongnian Du[1,2,3,4], Yang Liu[2,5], Lingpeng Liu[1,2,3,4], Jiajuan Li[1,2,3,4], Zehao Chen[1,2,3,4], Xuzhe Yu[1,2,3,4], Miao Ye[1,2,3,4], Wei Wang[1,2,3,4], Zijing Li[1,2,3,4] and Jianghua Shao[1,2,3,4,6*]

Abstract

Background Research has elucidated that homeobox B9 (HOXB9), an important transcriptional activator, plays a pivotal role in promoting the invasion and metastasis of hepatocellular carcinoma (HCC) cells. However, the mechanism by which HOXB9 promotes the invasion and metastasis of HCC cells is incompletely understood and needs further exploration.

Methods HOXB9 and snail family transcriptional repressor 2 (SNAI2) expression were analyzed using qRT-PCR and western blotting. The invasion and metastasis of hepatocellular carcinoma (HCC) cells were investigated using in vitro and in vivo assays. The H3K27me3 enrichment and HOXB9 interaction with microRNA 203a (MIR203A) or SNAI2 were detected using ChIP-qPCR. Transcriptional activities of *SNAI2* and *MIR203A* promoter were detected using dual-luciferase reporter assays. Co-IP and GST pull-down assays were performed to confirm the binding between HOXB9 and EZH2.

Results HOXB9 and SNAI2 were highly expressed in HCC tissues and their expression was positively intercorrelated and associated with poor prognosis in patients with HCC. In vitro and in vivo experiments confirmed that HOXB9 can upregulate the expression of SNAI2 to promote the invasion and metastasis of HCC cells. Furthermore, HOXB9 elevated SNAI2 expression by inhibiting *MIR203A* expression, a tumor suppressor gene, in HCC cells. Mechanistically, HOXB9 recruited enhancer of zeste 2 polycomb repressive complex 2 subunit (EZH2) through interaction with its WD-binding domain, which increased EZH2-mediated histone H3 lysine 27 trimethylation (H3K27me3) at the *MIR203A* promoter region, in turn repressing the transcriptional activity and expression of *MIR203A* and consequently increasing the SNAI2 level in HCC cells. Finally, empirical evidence from in vitro and in vivo studies confirmed that mitigation of the HOXB9-mediated enhancement of epigenetic silencing of *MIR203A* inhibited SNAI2 expression, impeding the invasion and metastasis of HCC cells.

Conclusions Our study reveals a novel mechanism by which HOXB9 promotes the invasion and metastasis of HCC cells and expands the understanding of the function of HOXB9 in tumor progression and provides a novel therapeutic strategy for curtailing HCC invasion and metastasis.

Keywords HOXB9, SNAI2, MIR203A, EZH2, H3K27me3, Invasion and metastasis, Hepatocellular carcinoma cells

†Dandan Zhang and Yumin Qiu contributed equally to this manuscript.

*Correspondence:
Jianghua Shao
shao5022@163.com
Full list of author information is available at the end of the article

Introduction

Hepatocellular carcinoma (HCC) is the sixth most prevalent cancer and the third leading cause of cancer-related mortality worldwide [1]. Despite substantial advances in the diagnosis and treatment of HCC, the prognosis for patients with HCC remains dismal, primarily due to tumor cell metastasis, thus posing a considerable global health challenge [2, 3]. Therefore, a deeper understanding of the molecular mechanisms promoting tumor invasion and metastasis in HCC is crucial for improving the survival and quality of life of patients with HCC.

Homeobox (*Hox*) genes, initially identified in the fruit fly *Drosophila melanogaster*, are characterized by a highly conserved 60-amino-acid motif known as the homeodomain and this domain is responsible for binding to DNA at specific recognition sites, leading to the transcriptional upregulation of their target genes [4–6]. Homeobox B9 (*HOXB9*) gene, a member of the *Hox* gene family, plays a pivotal role in cell proliferation and differentiation and is essential for embryonic segmentation [7]. Beyond its fundamental role in embryonic development, HOXB9 has been implicated in the progression of various tumors [8–10]. Elevated expression of HOXB9 is associated with poor clinical outcomes in different cancer types, including HCC [10–14]. Recently, the role of HOXB9 in promoting tumor invasion and metastasis in HCC has attracted increased attention. HOXB9 can activate various signaling pathways to promote the invasion and metastasis of HCC cells [15, 16]. In addition, we previously confirmed that the ubiquitin-like protein FAT10 upregulates HOXB9 expression by modulating β-catenin expression to promote the invasion and metastasis of HCC cells [17]. However, the mechanism by which HOXB9 promotes the invasion and metastasis of HCC cells remains unclear and requires further exploration.

Snail family transcriptional repressor 2 (SNAI2, also referred to as Slug) is a crucial member of the SNAI transcription factor family [18]. Elevated expression of SNAI2 has been observed in multiple cancers and is positively linked to a shorter survival time and increased risks of recurrence and metastasis in patients [19, 20]. High levels of SNAI2 expression enhance the invasion and metastasis of various cancers, including HCC [21–24]. Recent studies have reported that the non-coding RNA microRNA 203a (*MIR203A*), a tumor suppressor gene, plays an important role in regulating the expression of SNAI2 in tumor cells [25–27]. The expression of *MIR203A* is low in HCC cells, and increased *MIR203A* expression can lead to inhibition of SNAI2 expression to suppress the invasion and metastasis of HCC cells [28, 29]. Despite the relatively low expression of *MIR203A* in HCC cells, the causes of its downregulation remain poorly understood. In addition, research has suggested that enhancer of zeste 2 polycomb repressive complex 2 subunit (EZH2), a key histone methyltransferase, can promote histone H3 lysine 27 trimethylation (H3K27me3) in the promoter regions of *miRNAs*, resulting in epigenetic silencing of tumor suppressor gene *miRNAs* in tumor cells [30–32]. Thus, it is worth exploring whether the promoter region of the tumor suppressor gene *MIR203A* is also subject to EZH2-mediated H3K27me3 in HCC cells and, if so, what the underlying mechanism is.

In this study, we found that HOXB9 can inhibit the expression of *MIR203A* by recruiting EZH2 to increase H3K27me3 in the *MIR203A* promoter region, in turn upregulating the expression of SNAI2 and thereby promoting the invasion and metastasis of HCC cells.

Materials and methods

Patients and tumor specimens

All procedures conformed to the principles set forth by the Declaration of Helsinki. HCC tissues and normal liver tissue specimens were obtained from 128 patients with HCC who were admitted to the Department of General Surgery, the Second Affiliated Hospital of Nanchang University. Fresh tumor tissues were collected at the time of surgery, validated by pathological diagnosis, immediately snap-frozen in liquid nitrogen, and stored at − 80 °C for further analysis. The protocols for the collection of human tissue in the study were approved by the Ethics and Research Committees of the Second Affiliated Hospital of Nanchang University ([2015 No. (058)]).

Cell cultures

The following cell lines were purchased from the American Type Culture Collection (Manassas, VA, USA): normal human liver cells (HL7702); the human HCC lines Hep3B, Huh-7, HCCLM3, SK-HEP1, Li-7, and HepG2; and embryonic kidney HEK293T cells. All cell lines were authenticated by the Cell Bank using short tandem repeat profiling, and a mycoplasma detection kit (Shanghai GeneChem Co., Ltd.) was used to confirm the absence of mycoplasma contamination. All cell lines were routinely maintained in Dulbecco's modified Eagle's medium (DMEM; Gibco, Grand Island, NY, USA) supplemented with 10% fetal bovine serum (FBS; Gibco, Grand Island, NY, USA) at 37 °C in a humidified atmosphere containing 5% CO_2.

Western blot and Co-IP

For western blot, total protein was extracted from cells or tumor specimens, and equal amounts of protein were separated via sodium dodecyl sulfate–polyacrylamide gel electrophoresis (SDS-PAGE). Proteins were transferred to a nitrocellulose filter (Millipore, Bedford, MA, USA) by electroblotting. The membranes were then incubated

with primary antibodies according to the manufacturer's instructions. After a night of incubation at an appropriate concentration of 4 °C, the membranes were then washed with 1×TBST three times and incubated with the appropriate secondary antibodies. Then, specific antibody interactions were visualized by enhanced chemiluminescence (Thermo, Waltham, MA, USA). The intensity of each band was measured using Quantity-One software (Bio-Rad, Hercules, CA, USA).

For Co-IP, the cells were lysed in cell lysis buffer for western blot and IP (Beyotime Biotechnology, 20 mM Tris, pH 8.0, 150 mM NaCl, 5 mM EDTA, and 1% Triton X-100) and centrifuged at 12,000 rpm for 15 min to remove debris. 60 μL cleared lysates were used as the input group, and the remaining lysates were subjected to immunoprecipitation with antibodies. Rolling was performed at 4 °C overnight. Then, protein A/G PLUS-Agarose (Santa Cruz Biotechnology Cat# sc-2003, RRID: AB_10201400) was added, and the plate was allowed to rest for 6 h. Washing was performed three times with a Wash Buffer. Then, the appropriate Bis–Tris Gel was used for SDS-PAGE and western blot analysis.

Chromatin immunoprecipitation

Chromatin immunoprecipitation assays were performed using a SimpleChIP® Enzymatic Chromatin IP Kit (Cell Signaling Technology, #9003) as described. Briefly, 270 μL of 37% formaldehyde was added to cells suspended in 10 mL of medium to crosslink proteins to DNA at room temperature and crosslinked with 0.125 M glycine for 5 min. The chromatin was isolated by adding a lysis buffer, and the cells were disrupted with a Dounce homogenizer. Lysates were sonicated, the DNA was sheared to an average length of 150–600 bp, and the DNA concentration should ideally be between 50 and 200 μg/mL. For optimal ChIP results, approximately 5 to 10 μg of digested, cross-linked chromatin was used per immunoprecipitation. Subsequently, 10% of the sonication-treated chromatin was termed "input" and 80% was used for immunoprecipitation with the target antibody and termed "IP". The remaining 10% was incubated with rabbit IgG or Histone H3 as a negative and postive control, termed "IgG" and "H3", respectively. The complex was precipitated with protein A/G magnetic beads overnight. Complexes were washed with low salt wash buffer, high salt wash buffer, LiCl wash buffer, and TE buffer, and the magnetic beads were eluted in elution buffer with protease K at 65 °C for 2 h to reverse cross-links and obtain purified ChIP DNA. For ChIP-sequencing (ChIP-Seq), we contacted a technical service company for DNA sequencing. Briefly, ChIP-grade DNA was sequenced for data analysis after a series of steps, including initial quality control, sequencing library preparation, cluster generation, and sequencing. For ChIP-quantitative real-time PCR (ChIP-qPCR), the immunoprecipitated DNA fragments were analyzed by real-time PCR with primers. The primers used for qPCR were *MIR203A* from GENEPHARMA. The primers used were as follows: *MIR203A*, 5′-CCTGTACAATGGGCT GTGTG-3′ and 5′-GCTCTAGCTGCACTCACCTG-3′. The enrichment levels were calculated using the following formula: Fold Enrichment = $2^{(-\Delta\Delta Ct\ [ChIP/NIS])}$.

Transwell assays

Migration and invasion assays were performed using a Transwell system (8-μm pore size; BD Biosciences, NJ, USA). In brief, 5×10^4 cells resuspended in DMEM were seeded into the upper chambers, which were either uncoated (for the migration assay) or coated with Matrigel (BD Biosciences, Franklin Lakes, NJ, USA) (for the invasion assay). The lower chambers were filled with medium containing 15% FBS. After incubation for the indicated periods, the upper chambers were removed, and the cells on the lower surface of the membrane were fixed, stained with 0.1% crystal violet, and photographed. Cells were manually counted in five random visual fields per chamber.

Statistical analysis

All the data are expressed as the mean ± standard deviation. Differences between two groups were analyzed by Student's t test, and differences among more than two groups were evaluated by one-way analysis of variance (ANOVA) followed by Tukey's multiple comparison test. The Kaplan–Meier method was used to generate survival curves, and the log-rank test was used to determine the significance of differences in survival. *P* values less than 0.05 were considered to indicate statistical significance. Statistical analyses were conducted using GraphPad Prism software 9.0.

Results

Both HOXB9 and SNAI2 are upregulated in HCC tissues and are closely associated with poor prognosis

Analysis of RNA sequencing (RNA-seq) data from three independent sets of tissues from pathologically diagnosed HCC patients revealed that the mRNA levels of *HOXB9* and *SNAI2* were increased in HCC tissues compared with adjacent nontumor tissues (Fig. 1A). Further data analysis showed that the *SNAI2* expression was significantly increased in the *HOXB9* high expression group (Fig. 1B). In addition, the examination of the mRNA expression of *HOXB9* and *SNAI2* in 48 HCC tissues and the corresponding adjacent tissues using quantitative reverse transcription–polymerase chain reaction (qRT-PCR) revealed that *HOXB9* and *SNAI2* were upregulated in HCC tissues (Fig. 1C). Importantly, their

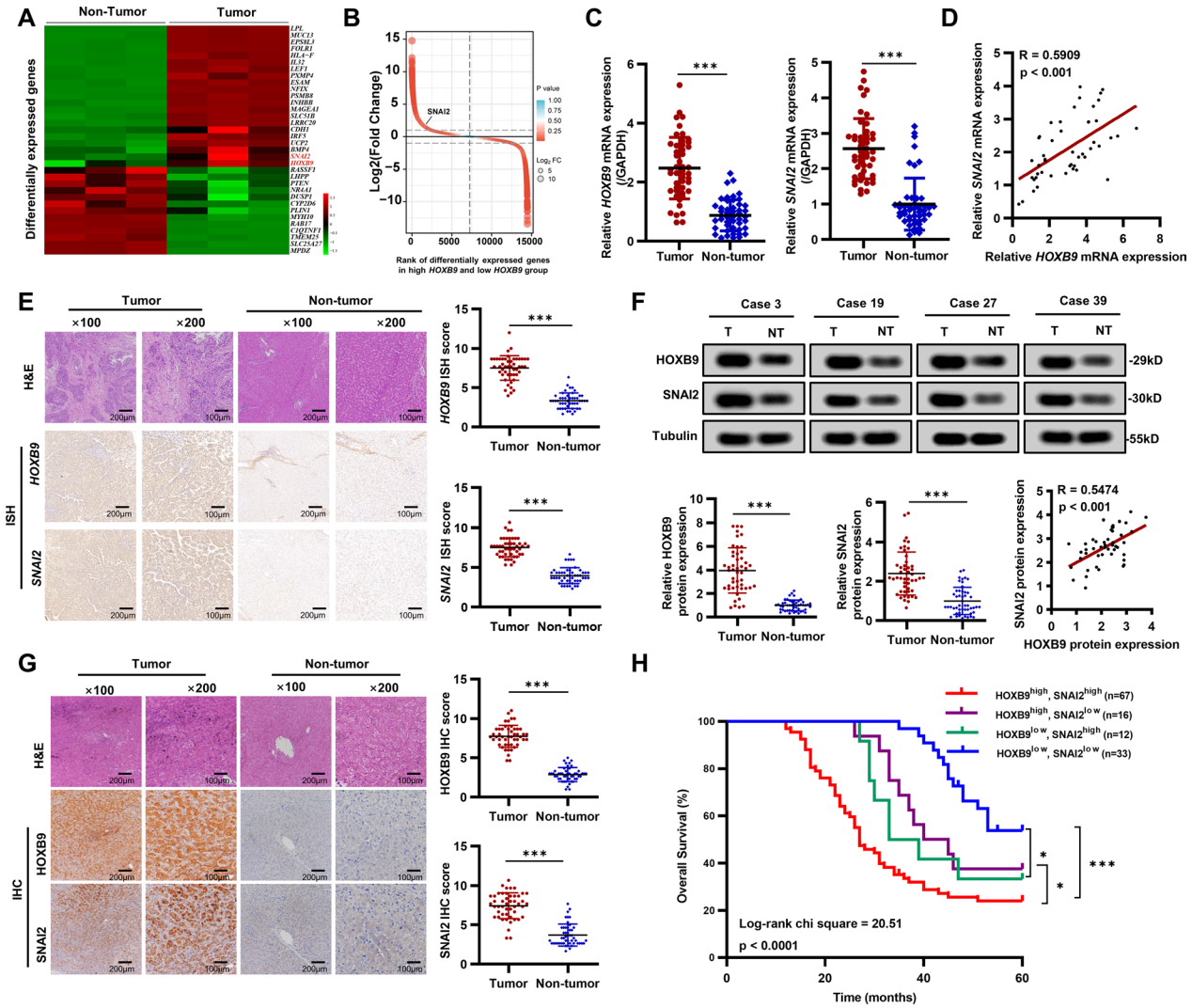

Fig. 1 HOXB9 and SNAI2 expression are upregulated in HCC tissues and are associated with poor prognosis. **A** HCC tissues and adjacent nontumor tissue samples were subjected to RNA-sequencing (RNA-seq) analysis (n = 3). **B** Rank of differentially expressed genes between high *HOXB9* and low *HOXB9* group. **C** qRT-PCR analysis detected the mRNA expression levels of *SNAI2* and *HOXB9* in paired HCC tissues and adjacent nontumor tissues (n = 48). **D** Scatter plots showed a positive correlation between *HOXB9* and *SNAI2* at the mRNA level in HCC tissues (n = 48). **E** Representative ISH staining and quantitative analysis of *SNAI2* and *HOXB9* in paired HCC tissues and adjacent nontumor tissues (n = 48). Scale bars = 200 μm and 100 μm. **F** Determination and quantification of HOXB9 and SNAI2 protein levels in paired HCC tissues and adjacent nontumor tissues by western blot assay (n = 48). Scatter plots showed a positive correlation between HOXB9 and SNAI2 at the protein level in HCC tissues. **G** Representative IHC staining and quantitative analysis of HOXB9 and SNAI2 protein expression in 48 pairs of HCC tissues and adjacent nontumor tissues (n = 48). Scale bars = 200 μm and 100 μm. **H** Kaplan–Meier curves for overall survival based on the combination of HOXB9 and SNAI2 protein levels. Patients diagnosed with HCC were divided into four groups based on HOXB9 and SNAI2 protein expression: Group 1 (n = 67): high HOXB9 and high SNAI2 expression; Group 2 (n = 16): high HOXB9 and low SNAI2 expression; Group 3 (n = 12): low HOXB9 and high SNAI2 expression; and Group 4 (n = 33): low HOXB9 and low SNAI2 expression. Data are represented as the mean ± SD. *$p < 0.05$ and ***$p < 0.001$

expression levels were positively correlated (R = 0.5909, p < 0.001) (Fig. 1D). Consistent with the qRT-PCR findings, in situ hybridization (ISH) was used to evaluate *HOXB9* and *SNAI2* expression in HCC and adjacent nontumor tissues, and the results confirmed their upregulation (Fig. 1E). Additionally, western blot and immunohistochemical (IHC) analyses revealed higher protein expression of HOXB9 and SNAI2 in HCC tissues than in adjacent tissues (Fig. 1F, G). Western blot analysis also revealed HOXB9 and SNAI2 overexpression in the six tested HCC cell lines compared with the immortalized liver cell line HL7702 (Fig. S1A–D). These results indicated that HOXB9 and SNAI2 were highly expressed both in HCC tissues and HCC cells.

We then analyzed the correlations of HOXB9 and SNAI2 protein expression with clinicopathological parameters in 128 patients with HCC. Both HOXB9 and SNAI2 overexpression correlated closely with tumor venous invasion, TNM stage and tumor microsatellite formation (Table 1). Kaplan–Meier analysis revealed that patients with HCC with high HOXB9 and SNAI2 expression had the lowest overall survival rate, whereas those with low HOXB9 and SNAI2 expression had the highest overall survival rate (Fig. 1H). Overall, our results indicated that both HOXB9 and SNAI2 were significantly upregulated in HCC tissues and that this upregulation was associated with poor prognosis in patients with HCC.

HOXB9 upregulates the expression of SNAI2 to promote the invasion and metastasis of HCC cells

Our in vitro experiments demonstrated that reducing HOXB9 expression inhibited the migration and invasion of HCCLM3 cells by suppressing SNAI2 expression. qRT-PCR and western blot analyses revealed that HOXB9 knockdown decreased the mRNA and protein levels of *SNAI2* in HCCLM3 cells (Fig. S2A). Transwell assays and real-time cellular analysis (RTCA) revealed reductions in the migration and invasion capabilities of HCCLM3 cells with HOXB9 knockdown (Fig. S2B, C). Furthermore, rescue experiments indicated that HOXB9 downregulation decreased SNAI2 expression, whereas SNAI2 upregulation attenuated the decrease in SNAI2 expression caused by HOXB9 downregulation in HCCLM3 cells (Fig. 2A). Transwell assays also showed that HOXB9 knockdown dramatically decreased the migration and invasion abilities of HCCLM3 cells, whereas SNAI2 upregulation reversed the HOXB9 knockdown-induced decreases in the migration and invasion abilities (Fig. 2B). In contrast, HOXB9 overexpression increased migration and invasion by upregulating SNAI2 expression in Hep3B cells (Fig. S2D–F, Fig. 2C, D).

Furthermore, our in vivo experiments indicated that HOXB9 upregulated SNAI2 expression to promote the lung metastasis of HCC cells. Lung metastasis models were established in BALB/c nude mice via tail vein injection of shNC-HCCLM3 and shHOXB9-HCCLM3 cells. After four weeks, the images acquired with an in vivo imaging system (IVIS) indicated a significant reduction in the fluorescence intensity in the shHOXB9-HCCLM3 group compared with the shNC-HCCLM3 group (Fig. 2E). Hematoxylin and eosin (H&E) staining of lung tissues confirmed a significant decrease in the number of metastatic lung nodules in the shHOXB9-HCCLM3 group (Fig. 2F). IHC staining of lung metastases revealed decreased HOXB9 and SNAI2 protein levels in shHOXB9-HCCLM3 cells compared with shNC-HCCLM3 cells (Fig. 2G). Conversely, HOXB9 overexpression in Hep3B cells upregulated SNAI2 expression, promoting lung metastasis (Fig. 2H–J). Collectively, these findings

Table 1 Correlation of HOXB9 and SNAI2 with the clinicopathological features of 128 patients with HCC

Variables	Clinicopathological characteristics	HOXB9			SNAI2		
		High expression	Low expression	*P* value	High expression	Low expression	*P* value
Age	< 60	38	20	0.885	33	25	0.307
	≥ 60	45	25		46	24	
Gender	Female	26	10	0.274	19	17	0.193
	Male	57	35		60	32	
HBsAg	Negative	10	5	0.875	9	6	0.884
	Positive	73	40		70	43	
Tumor size	< 5 cm	37	26	0.154	43	20	0.134
	≥ 5 cm	46	19		36	29	
Venous invasion	Absent	22	25	**0.001****	23	24	**0.023***
	Present	61	20		56	25	
TNM stage	I–II	34	29	**0.011***	30	33	**0.001****
	III–IV	49	16		49	16	
Tumor microsatellite formation	Absent	19	23	**0.001****	20	22	**0.022***
	Present	64	22		59	27	
AFP	Normal	21	18	0.085	25	14	0.713
	Abnormal	62	27		54	35	

TNM Tumor node metastasis, *HBsAg* hepatitis B surface antigen, *AFP* Alpha-fetoprotein

*$p < 0.05$ and **$p < 0.01$ indicate significance. Bold values are statistically signifcant

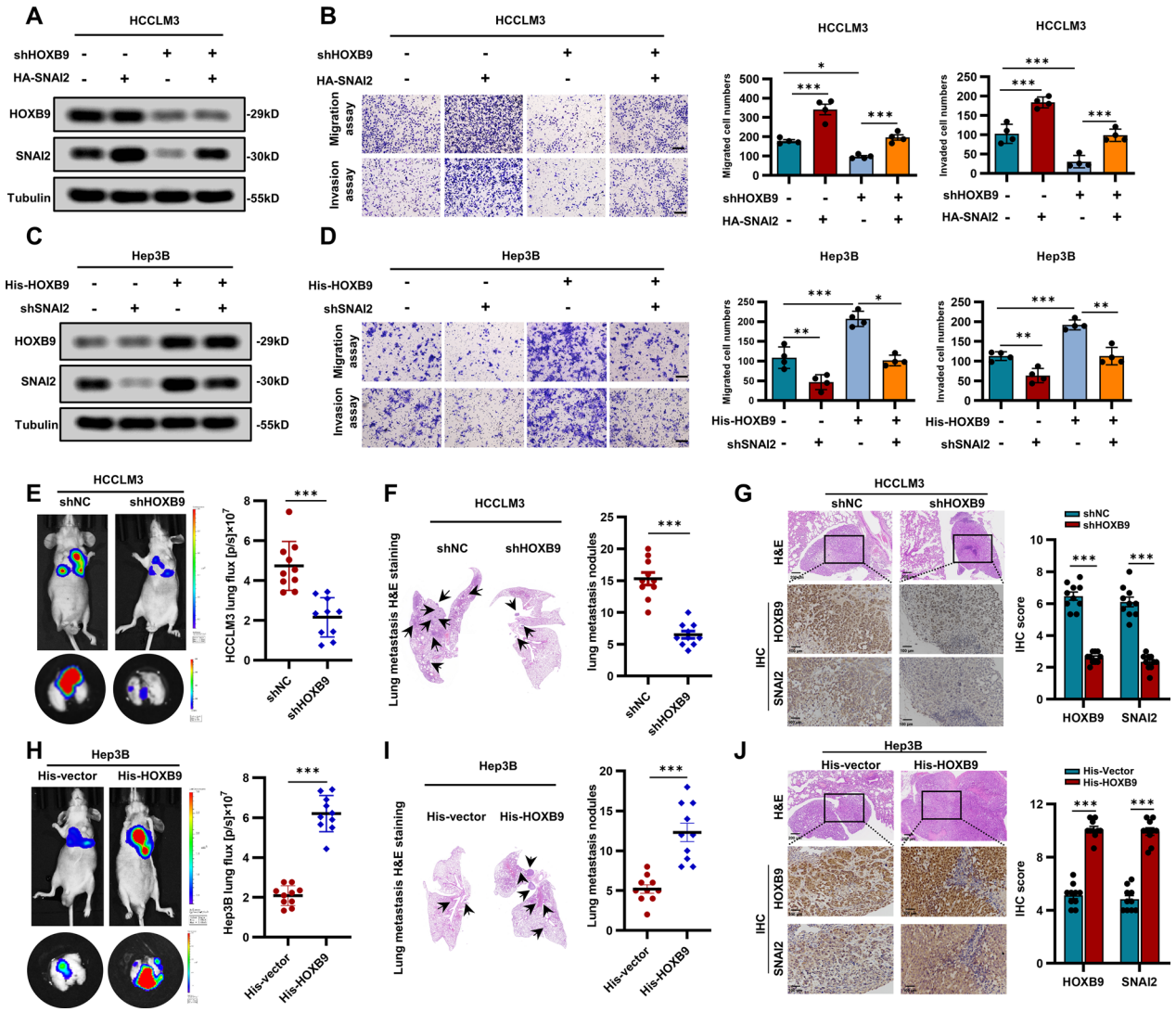

Fig. 2 HOXB9 upregulates the expression of SNAI2 to promote the invasion and metastasis of HCC cells. **A** Western blot was used to analyze the protein levels of HOXB9 and SNAI2 in HCCLM3 cells with the indicated treatments. **B** Transwell assays detected the migration and invasion capacities of HCCLM3 cells with the indicated treatments (n = 4). Scale bars = 100 μm. **C** Western blot analyzed the protein levels of HOXB9 and SNAI2 in Hep3B cells with the indicated treatments. **D** Transwell assays detected the migration and invasion capacities of Hep3B cells with the indicated treatments (n = 4). Scale bars = 100 μm. **E** and **F** Representative bioluminescent images and quantification analysis (**E**) of lung tumors in nude mice intravenously injected with HOXB9 knockdown HCCLM3 cells, and H&E-stained images and quantification analysis (**F**) of metastatic nodules in the lungs (n = 10 mice per group). **G** IHC analysis of HOXB9 and SNAI2 levels in metastatic pulmonary tumors in the above groups. Scale bars = 200 μm and 100 μm. **H** and **I** Representative bioluminescent images and quantification analysis of lung tumors (**H**) in nude mice intravenously injected with HOXB9 overexpression Hep3B cells, H&E-stained images and quantification analysis (**I**) of metastatic nodules in the lungs. (n = 10 mice per group). **J** IHC analysis of HOXB9 and SNAI2 expression levels in metastatic pulmonary tumors in the above groups. Scale bars = 200 μm and 100 μm. Data represent the mean ± SD. *$p < 0.05$, **$p < 0.01$ and ***$p < 0.001$

indicated that HOXB9 upregulated the expression of SNAI2 to promote the invasion and metastasis of HCC cells in vitro and in vivo.

HOXB9 upregulates SNAI2 expression by inhibiting MIR203A expression in HCC cells

The results of chromatin immunoprecipitation followed by sequencing (ChIP-seq) indicated that HOXB9 did not bind to the *SNAI2* promoter region in HCCLM3 cells (Fig. 3A). Moreover, the dual-luciferase reporter assay also showed that neither the downregulation nor

overexpression of HOXB9 affected the transcriptional activity of *SNAI2* promoter in HCCLM3 and Hep3B cells (Fig. 3B), suggesting that HOXB9 does not directly regulate *SNAI2* transcription; therefore, intermediate mediators that regulate the expression of SNAI2 induced by HOXB9 in HCC cells may exist. Previous studies have reported that *MIR203A* plays an important role in regulating the expression of SNAI2 in HCC cells [29]. Therefore, we sought to investigate whether HOXB9 can regulate SNAI2 expression by modulating the *MIR203A* level. We first found that reduced *MIR203A* expression led to upregulated SNAI2 expression, increasing the migration and invasion of HCC cells. Our results showed that increased *MIR203A* expression decreased the mRNA and protein levels of *SNAI2* to inhibit the migration and invasion of HCC cells in a dose-dependent manner (Fig. S3A–D). Conversely, decreased *MIR203A* expression resulted in an increase in the level of *SNAI2* to promote the migration and invasion of HCC cells (Fig. S3E–H).

Subsequent investigation focused on whether HOXB9 regulates SNAI2 expression by modulating *MIR203A* levels in HCC cells. We first found that HOXB9 can regulate *MIR203A* expression in HCC cells. miRNA sequencing (miRNA-seq) revealed increased *MIR203A* expression in shHOXB9-HCCLM3 cells compared with shNC-HCCLM3 cells (Fig. 3C). qRT-PCR revealed that HOXB9 downregulation led to elevated *MIR203A* expression in HCCLM3 cells, whereas HOXB9 upregulation suppressed *MIR203A* expression in Hep3B cells (Fig. 3D). Furthermore, rescue experiments showed that reducing HOXB9 expression increased the *MIR203A* level and decreased mRNA and protein expression of *SNAI2*; however, *MIR203A* downregulation counteracted the increase in *MIR203A* expression and the reduction in *SNAI2* expression triggered by HOXB9 silencing in HCCLM3 cells (Fig. 3E). Consistently, RTCA and the transwell assays showed that concomitant *MIR203A* knockdown reversed the HOXB9 downregulation-induced reductions in the migration and invasion abilities of HCCLM3 cells (Fig. 3F, G). In contrast, HOXB9 overexpression reduced the *MIR203A* level, thereby increasing *SNAI2* expression and augmenting the migratory and invasive capacities of Hep3B cells (Fig. 3H–J). Thus, these results indicated that HOXB9 can upregulate the expression of SNAI2 by inhibiting *MIR203A* expression in HCC cells.

HOXB9 increases H3K27me3 of the MIR203A promoter to inhibit its transcriptional activity in HCC cells

We then explored the mechanism by which HOXB9 inhibits *MIR203A* expression in HCC cells. The chromatin isolation by RNA purification sequencing (ChIRP-seq) results showed that HOXB9 had an enrichment peak in the upstream promoter region (approximately 1,800 bp) of *MIR203A* in HCCLM3 cells (Fig. 4A). ChIP-qPCR results also revealed that HOXB9 could indeed be enriched in the promoter region of *MIR203A* in HCC cells (Fig. 4B, Fig. S4A). Furthermore, ChIP-qPCR and dual-luciferase reporter assay results showed that although HOXB9 overexpression increased the enrichment of HOXB9 in the *MIR203A* promoter region, the transcriptional activity of the *MIR203A* promoter was inhibited in HCC cells (Fig. 4C, D, Fig. S4B, C). Conversely, HOXB9 knockdown decreased the enrichment of HOXB9 in the *MIR203A* promoter region, but the transcriptional activity of the *MIR203A* promoter was increased in HCC cells (Fig. 4E, F, Fig. S4D, E). These results indicated that HOXB9 overexpression can inhibit the transcriptional activity of the *MIR203A* promoter in HCC cells.

Studies have indicated that histone H3 methylation modifications, such as H3K27me3, H3K4me3 and H3K9me3, in promoter regions play important roles in regulating the transcriptional activity of miRNAs [33–35]. Thus, we further investigated the status of H3K27me3, H3K4me3 and H3K9me3 in the *MIR203A* promoter region in HCC cells overexpressing HOXB9. ChIP-qPCR results indicated that HOXB9 overexpression increased the enrichment of H3K27me3 in the *MIR203A* promoter region, whereas no significant changes were observed in the enrichment of H3K4me3 and H3K9me3

(See figure on next page.)

Fig. 3 HOXB9 upregulates SNAI2 expression by inhibiting *MIR203A* expression in HCC cells. **A** The ChIP-seq signal for HOXB9 at SNAI2 loci in HCCLM3 cells. The ChIP-seq signal was normalized to the sequencing depth to make samples comparable. **B** The relative luciferase activity of *SNAI2* promoter in HCCLM3 and Hep3B cells with the indicated treatments (n = 3). **C** Heatmap representation of differentially expressed miRNAs in the HCCLM3 with HOXB9 knockdown cells ($p < 0.05$ and FC > 1.5). Upregulated miRNAs were shown in red, while downregulated miRNAs were shown in green. Row, miRNA; columns, independent biological replicates (n = 3). **D** qRT-PCR detected *MIR203A* expression after changing HOXB9 expression in HCCLM3 and Hep3B (n = 4). **E** qRT-PCR detected mRNAs of *MIR203A* and *SNAI2* in HCCLM3 cells with the indicated treatments (n = 4) and western blot analyzed the protein levels of HOXB9 and SNAI2 in the above different groups. **F** and **G** RTCA (**F**) and transwell assays (**G**) were used to detect the invasion and migration abilities of HCCLM3 cells with the indicated treatments (n = 4). Scale bars = 100 μm. **H** qRT-PCR detected mRNAs of *MIR203A* and *SNAI2* in Hep3B cells with the indicated treatments (n = 4) and western blot showed the protein levels of HOXB9 and SNAI2 in the above different groups. **I** and **J** RTCA (**I**) and transwell assays (**J**) detected the invasion and migration abilities of Hep3B cells with the indicated treatments (n = 4). Scale bars = 100 μm. Data represent the mean ± SD. ns, $p > 0.05$, *$p < 0.05$, **$p < 0.01$ and ***$p < 0.001$

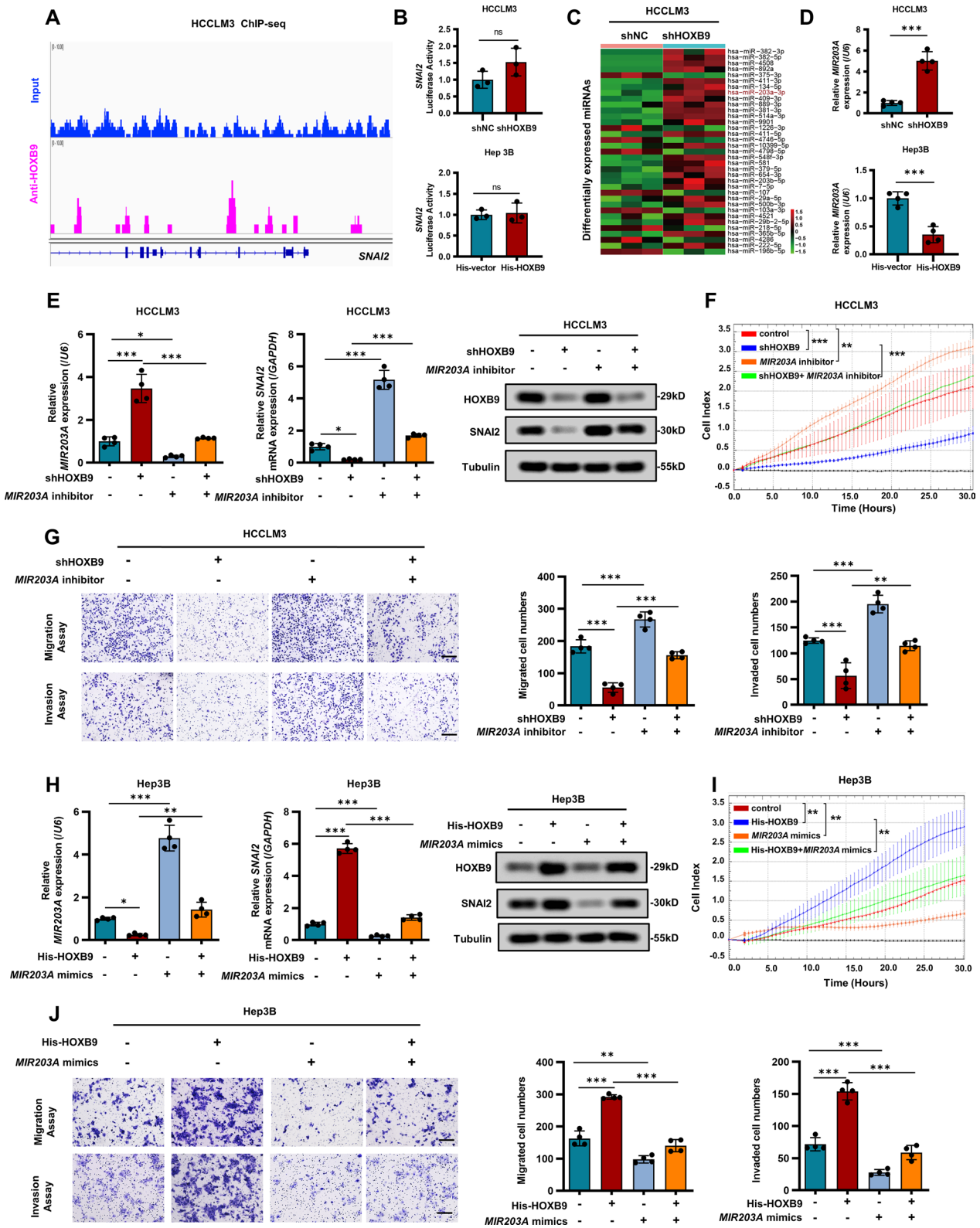

Fig. 3 (See legend on previous page.)

in HCCLM3 cells (Fig. 4G). ChIP-qPCR further showed that HOXB9 downregulation led to decreased enrichment of H3K27me3 in the *MIR203A* promoter region in HCCLM3 cells (Fig. 4H). ChIP-qPCR also revealed that the enrichment of H3K27me3 in the *MIR203A* promoter region changed along with changes in HOXB9 expression in Hep3B cells (Fig. S4F, G). These results indicated that HOXB9 overexpression increases the H3K27me3 level in the *MIR203A* promoter region in HCC cells.

Furthermore, we investigated whether HOXB9 can increase H3K27me3 in the *MIR203A* promoter region to inhibit the transcriptional activity of the *MIR203A* promoter in HCC cells. ChIP-qPCR revealed that HOXB9 overexpression increased the enrichment of H3K27me3 in the *MIR203A* promoter region in HCC cells, and dual-luciferase reporter assays and qRT-PCR analyses revealed that HOXB9 overexpression inhibited the transcriptional activity and expression of *MIR203A* in HCC cells; however, treatment with 3-deazaneplanocin (DZNeP), an inhibitor of H3K27me3, attenuated the increase in H3K27me3 enrichment in the *MIR203A* promoter region and the inhibition of *MIR203A* transcriptional activity and expression caused by HOXB9 overexpression in HCC cells (Fig. 4I–K, Fig. S4H–J). Overall, our results confirmed that HOXB9 overexpression can increase the H3K27me3 level in the *MIR203A* promoter region, leading to inhibition of the transcriptional activity of the *MIR203A* promoter in HCC cells.

HOXB9-mediated increase in H3K27me3 in the MIR203A promoter to inhibit its transcriptional activity depends on EZH2 in HCC cells

Previous studies have indicated that the EZH2-mediated increase in H3K27me3 in miRNA promoter regions plays an important role in inhibiting the transcriptional activity of miRNA promoters in tumor cells [30, 36]. Therefore, we further sought to determine whether EZH2 is involved in the HOXB9-mediated increase in H3K27me3 in the *MIR203A* promoter region in HCC cells. Our results first confirmed that EZH2 increased the H3K27me3 level in the *MIR203A* promoter region to inhibit the transcriptional activity and expression of *MIR203A* in HCCLM3 and Hep3B cells. ChIP-qPCR indicated that EZH2 upregulation increased the enrichment of both EZH2 and H3K27me3 in the *MIR203A* promoter region; however, dual-luciferase reporter assays and qRT-PCR demonstrated that EZH2 upregulation decreased the transcriptional activity and expression of *MIR203A* in HCC cells (Fig. 5A–C, Fig. S5A–C). The opposite effects were observed in HCC cells with EZH2 knockdown (Fig. 5D–F, Fig. S5D–F).

Next, our results confirmed that the HOXB9-mediated increase in H3K27me3 in the *MIR203A* promoter region inhibited the transcriptional activity of *MIR203A* through EZH2 in HCC cells. Notably, modifying HOXB9 expression did not affect the mRNA or protein level of *EZH2* in HCC cells (Fig. 5G, Fig. S5G). However, HOXB9 overexpression increased the H3K27me3 level in the promoter region of *MIR203A*, accompanied by decreases in the transcriptional activity and expression of *MIR203A* in HCC cells, and EZH2 downregulation attenuated the above changes caused by HOXB9 overexpression in HCC cells (Fig. 5H–J, Fig. S5H–J). Furthermore, we used GSK126, an EZH2 methyltransferase inhibitor, and the results of these rescue experiments showed that GSK126 did not alter the mRNA or protein expression level of *HOXB9* or *EZH2* but did attenuate the increase in the H3K27me3 level in the promoter region of *MIR203A* and the decreases in the transcriptional activity and expression of *MIR203A* caused by HOXB9 overexpression in HCC cells (Fig. 5K–N, Fig. S5K–N).

Furthermore, we explored whether the HOXB9-induced increase in H3K27me3 in the *MIR203A* promoter region in HCC cells is dependent on EZH2. To this end, *EZH2* knockout HCCLM3 ($EZH2^{-/-}$ HCCLM3) cells were engineered utilizing the CRISPR-Cas9 system (Fig. S6A, B). Next, the expression of HOXB9 in $EZH2^{-/-}$ HCCLM3 cells was altered; western blot results showed

(See figure on next page.)

Fig. 4 HOXB9 inhibits the transcriptional activity of *MIR203A* by enhancing its promoter H3K27me3 in HCC cells. **A** ChIRP-seq signal for HOXB9 at *MIR203A* loci in HCCLM3 cells and the ChIP-seq signal was normalized to the sequencing depth to make samples comparable. **B** ChIP-qPCR showed the enrichment level of HOXB9 at the *MIR203A* promoter region in HCCLM3 (n = 4). **C** and **D** The enrichment level of HOXB9 at the *MIR203A* promoter region (**C**) and the relative transcriptional activity of the *MIR203A* (**D**) in HCCLM3 cells with HOXB9 overexpression were determined by using ChIP-qPCR and dual-luciferase reporter assay, respectively (n = 4). **E** and **F** ChIP-qPCR detected the enrichment level of HOXB9 at the *MIR203A* promoter region in HCCLM3 cells with HOXB9 knockdown (**E**), and dual-luciferase reporter assay detected the relative transcriptional activity of *MIR203A* (**F**) in the above different groups (n = 4). **G** ChIP-qPCR detected the enrichment levels of H3K4me3, H3K9me3, and H3K27me3 at the *MIR203A* promoter in HCCLM3 cells with HOXB9 overexpression (n = 4). **H** ChIP-qPCR detected the enrichment level of H3K27me3 at the *MIR203A* promoter in HCCLM3 cells with knockdown HOXB9 (n = 4). **I** The enrichment level of H3K27me3 at the *MIR203A* promoter in HCCLM3 cells with the indicated treatments was detected by ChIP-qPCR (n = 4). **J** and **K** The transcriptional activity of the *MIR203A* (**J**) and the *MIR203A* expression levels (**K**) in HCCLM3 cells with the indicated treatments were detected by dual-luciferase reporter assay and qRT-PCR, respectively (n = 4). Data represent the mean ± SD. ns, $p > 0.05$, *$p < 0.05$, **$p < 0.01$ and ***$p < 0.001$

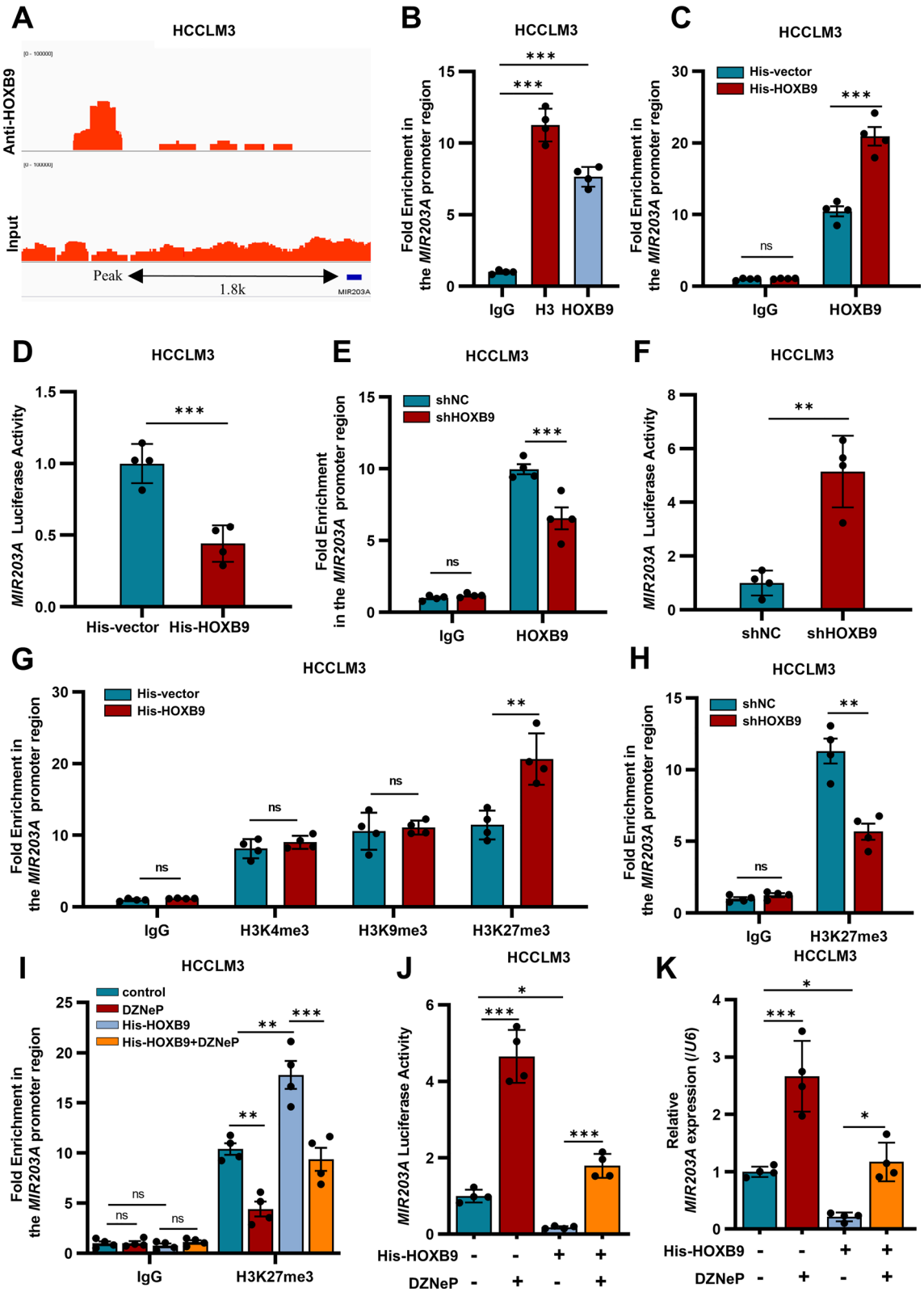

Fig. 4 (See legend on previous page.)

that the protein level of HOXB9 varied as the HOXB9 expression changed compared with the control group in *EZH2*$^{-/-}$ HCCLM3 cells and ChIP-qPCR results showed that the enrichment level of H3K27me3 in the *MIR203A* promoter region remained unchanged, regardless of the changes in the expression levels of HOXB9 in *EZH2*$^{-/-}$ HCCLM3 cells (Fig. 5O, P). Dual-luciferase reporter assays and qRT-PCR showed that HOXB9 downregulation inhibited the transcriptional activity and expression of *MIR203A*, whereas HOXB9 upregulation increased the transcriptional activity and expression of *MIR203A* in *EZH2*$^{-/-}$ HCCLM3 cells (Fig. 5Q). However, the opposite patterns were observed in *EZH2*$^{-/-}$ HCCLM3 cells transfected with the Flag-EZH2 plasmid (Fig. 5R–T). Hence, these results confirmed that HOXB9-mediated increase in H3K27me3 in the *MIR203A* promoter region, which resulted in inhibition of the transcriptional activity of the *MIR203A* promoter, was dependent on EZH2 in HCC cells.

HOXB9 recruits EZH2 to enhance the epigenetic silencing of MIR203A and thereby promotes SNAI2 expression in HCC cells

A previous study suggested that transcription factors can bind to EZH2, subsequently recruiting it to increase the H3K27me3 level in the promoter regions of target gene [37]. Therefore, we speculated that HOXB9 can also recruit EZH2 to increase the H3K27me3 level in the *MIR203A* promoter region in HCC cells. Our results first revealed that HOXB9 can bind to the WD-binding (WDB) domain of EZH2 in HCC cells. Co-immunoprecipitation (Co-IP) and confocal immunofluorescence assays revealed the interaction and co-localization of HOXB9 with EZH2 in HCC cells (Fig. 6A, B, Fig. S7A, B). Glutathione S-transferase (GST) pulldown and Co-IP assays confirmed that HOXB9 directly bound to the N-terminal WDB domain of EZH2 (Fig. 6C–E). Moreover, Co-IP assays confirmed that the WDB domain of EZH2 is essential for its binding to HOXB9 in HCCLM3 cells (Fig. 6F). Furthermore, our results revealed that HOXB9 overexpression increased the binding between HOXB9 and EZH2, accompanied by increased H3K27me3 enrichment in the *MIR203A* promoter region, which resulted in inhibition of the transcriptional activity and expression of *MIR203A* in HCC cells. Co-IP and ChIP-qPCR results showed that HOXB9 downregulation decreased the binding between HOXB9 and EZH2, decreased H3K27me3 enrichment in the *MIR203A* promoter region; whereas HOXB9 upregulation increased the binding between HOXB9 and EZH2, increased H3K27me3 enrichment in the *MIR203A* promoter region (Fig. 6G, H, Fig. S7C, D). The results of dual-luciferase reporter assay and qRT-PCR demonstrated that HOXB9 downregulation increased the transcriptional activity and expression of *MIR203A*; whereas HOXB9 upregulation decreased the transcriptional activity and expression of *MIR203A* (Fig. 6I, Fig. S7E). These results confirmed that HOXB9 can recruit EZH2 by binding to the WDB domain of EZH2 to increase the H3K27me3 level in the *MIR203A* promoter region in HCC cells.

Hence, consolidating all the preceding results, we hypothesized that HOXB9 upregulates SNAI2 expression through the recruitment of EZH2, leading to increased binding between HOXB9 and EZH2, which enhances the epigenetic silencing of *MIR203A*. This silencing, in turn, inhibits the transcriptional activity and expression of *MIR203A*, subsequently upregulating SNAI2 expression in HCC cells. To confirm this hypothesis, we altered the expression of HOXB9 and then investigated the binding of HOXB9 to EZH2, the H3K27me3 level in the *MIR203A* promoter region, the transcriptional activity and expression levels of *MIR203A*, and the SNAI2 level in

(See figure on next page.)

Fig. 5 HOXB9-enhanced H3K27me3 in the *MIR203A* promoter region depends on EZH2 in HCC cells. **A** qRT-PCR and western blot analyzed the *EZH2* mRNA and protein levels (n = 4). **B** and **C** The enrichment levels of EZH2 and H3K27me3 at the *MIR203A* promoter (**B**), the transcriptional activity and expression of *MIR203A* (**C**) were detected (n = 4). **D** qRT-PCR and western blot analyzed the *EZH2* mRNA and protein levels (n = 4). **E** and **F** The enrichment levels of EZH2 and H3K27me3 at the *MIR203A* promoter (**E**), the transcriptional activity and expression of *MIR203A* (**F**) were analyzed (n = 4). **G** qRT-PCR and western blot were used to analyze the mRNA and protein levels of *EZH2* and *HOXB9* (n = 4). **H** qRT-PCR and western blot were used to analyze the mRNA and protein levels of *EZH2* and *HOXB9* (n = 4). **I** and **J** H3K27me3 enrichment at the *MIR203A* promoter (**I**), the transcriptional activity and expression of *MIR203A* (**J**) were detected (n = 4). **K** and **L** qRT-PCR (**K**) and western blot (**L**) were used to analyze the mRNA and protein levels of *EZH2* and *HOXB9* in HCCLM3 cells (n = 4). **M** and **N** The H3K27me3 enrichment at the *MIR203A* promoter (**M**), the transcriptional activity and expression of *MIR203A* (**N**) were detected in different groups (n = 4). **O** Western blot was used to analyze the protein levels of EZH2 and HOXB9 after changing HOXB9 in *EZH2*$^{-/-}$ HCCLM3 cells. **P** ChIP-qPCR was used to explore the H3K27me3 enrichment at the *MIR203A* promoter region in *EZH2*$^{-/-}$ HCCLM3 cells with the indicated treatments (n = 4). **Q** Dual-luciferase reporter assay and qRT-PCR detected transcriptional activity of the *MIR203A* promoter and *MIR203A* levels in different groups (n = 4). **R** Western blot analyzed the protein levels of EZH2 and HOXB9 after changing HOXB9 in *EZH2*$^{-/-}$ HCCLM3 cells transfected with the Flag-EZH2 plasmid (n = 4). **S** ChIP-qPCR explored H3K27me3 enrichment at the *MIR203A* promoter region after changing HOXB9 in different groups (n = 4). **T** Dual-luciferase reporter assay and qRT-PCR detected transcriptional activity of the *MIR203A* promoter and *MIR203A* levels in different groups (n = 4). Data are represented as the mean ± SD. ns, $p > 0.05$, *$p < 0.05$, **$p < 0.01$ and ***$p < 0.001$

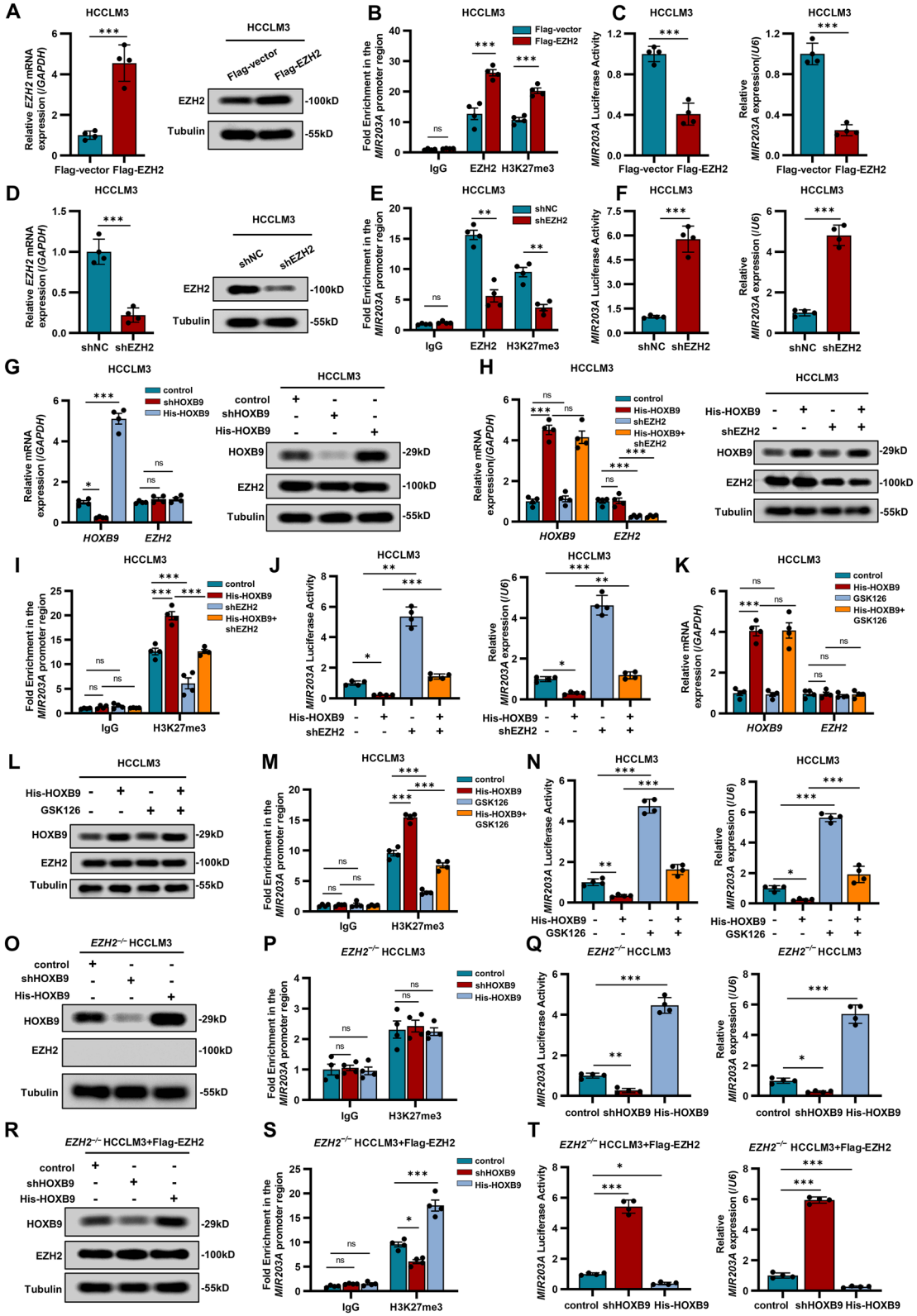

Fig. 5 (See legend on previous page.)

HCC cells. Co-IP assays revealed that with the upregulation of HOXB9, the intensity of binding between HOXB9 and EZH2 increased, and concomitantly, the SNAI2 protein level also increased in a dose-dependent manner in HCC cells (Fig. 6J, Fig. S7F). Although the ChIP-qPCR results showed that the enrichment of H3K27me3 in the *MIR203A* promoter region increased gradually with HOXB9 upregulation, the dual-luciferase reporter assay showed that the transcriptional activity of the *MIR203A* promoter gradually decreased in HCC cells (Fig. 6K, L, Fig. S7G, H). Moreover, qRT-PCR results showed that the expression level of *MIR203A* gradually decreased and the mRNA level of *SNAI2* gradually increased as HOXB9 expression increased in HCC cells (Fig. 6M, Fig. S7I). Conversely, downregulation of HOXB9 reduced the binding of HOXB9 to EZH2 and the H3K27me3 level in the *MIR203A* promoter region, increased the transcriptional activity of the *MIR203A* promoter and *MIR203A* expression, and decreased the mRNA and protein levels of *SNAI2* in HCC cells (Fig. 6N–Q, Fig. S7J–M). Overall, our results confirmed that HOXB9 can recruit EZH2 to enhance the epigenetic silencing of *MIR203A* and thereby promoted SNAI2 expression in HCC cells.

GSK126 mitigates the HOXB9-mediated enhancement of MIR203A silencing and thereby downregulates SNAI2 to inhibit the invasion and metastasis of HCC cells

Given the important role of EZH2-mediated H3K27me3 in the regulation of the *MIR203A*-SNAI2 axis by HOXB9 in HCC cells, we explored whether alleviating the HOXB9-mediated enhancement of *MIR203A* silencing reduces SNAI2 expression to curtail the invasion and metastasis of HCC cells. To this end, we used GSK126 to inhibit EZH2-mediated H3K27me3 in HCC cells. ChIP-qPCR demonstrated that HOXB9 overexpression increased the H3K27me3 level in the *MIR203A* promoter region; however, GSK126 treatment decreased the promoting effect of HOXB9 on H3K27me3 in the *MIR203A* promoter region (Fig. 7A, Fig. S8A). Dual-luciferase reporter assays and qRT-PCR analysis also showed that GSK126 attenuated the decreases in the transcriptional activity of the *MIR203A* promoter and *MIR203A* expression caused by HOXB9 overexpression in HCC cells (Fig. 7B, Fig. S8B). Furthermore, qRT-PCR and western blot revealed that while HOXB9 overexpression increased the mRNA and protein levels of *SNAI2*, GSK126 treatment reversed these increases in HCC cells (Fig. 7C, Fig. S8C). Correspondingly, the results of transwell assays and RTCA illustrated that GSK126 treatment mitigated the increases in the migration and invasion capabilities induced by HOXB9 overexpression in HCC cells (Fig. 7D, E, Fig. S8D, E). These in vitro results confirmed that GSK126 counteracted HOXB9-promoted epigenetic silencing of *MIR203A*, leading to the downregulation of SNAI2 expression and impeding the migration and invasion of HCC cells.

Furthermore, our in vivo findings confirmed that GSK126 alleviated HOXB9-promoted epigenetic silencing of *MIR203A*, leading to the downregulation of SNAI2 expression and impeding the lung metastasis of HCC cells. Initially, we injected His-vector or His-HOXB9-HCC cells into BALB/c nude mice via the tail vein. After one week, we applied GSK126 treatment in the HOXB9 overexpressing group, with one subset receiving GSK126 treatment and another left untreated (Fig. 7F). Four weeks post-HCC cell injection, IVIS imaging and H&E staining of lung tissues revealed that HOXB9 overexpression significantly increased the fluorescence intensity in lung tissue and the number of lung metastatic nodules compared with those in the control group; however, both the fluorescence intensity in lung tissues and the number of lung metastatic nodules were significantly reduced in the GSK126-treated group compared to those in the untreated group (Fig. 7G, H, Fig. S8F, G). IHC analysis of lung metastases revealed that GSK126 treatment attenuated the increase in

(See figure on next page.)

Fig. 6 HOXB9 recruits EZH2 to enhance H3K27me3 of *MIR203A* and then promotes SNAI2 expression in HCC cells. **A** Co-IP detected the interaction between HOXB9 and EZH2 protein in HCCLM3 cells. **B** Confocal microscopy showing co-localization of HOXB9 and EZH2. Scale bar = 10 μm. **C** Schematic illustration showing the construction of full-length EZH2 and its truncations. **D** GST pull-down assay detected the interaction between full-length His-EZH2 purified proteins or EZH2 truncated purified proteins with GST-HOXB9 purified proteins. **E** HEK293T cells were transfected with the indicated constructs, and cells were lysed for Co-IP using anti-His beads to detect GST binding. **F** Cells were lysed for Co-IP using anti-GST beads to detect Flag binding. **G** Cells were lysed for Co-IP using anti-HOXB9 beads to detect HOXB9 binding to EZH2 following altered HOXB9 protein expression. **H** ChIP-qPCR was used to analyze the enrichment levels of HOXB9, EZH2 and H3K27me3 at the *MIR203A* promoter (n = 4). **I** The transcriptional activity of the *MIR203A* promoter and *MIR203A* expression were detected (n = 4). **J** Co-IP detected the interaction between HOXB9 and EZH2 in different groups. **K** and **L** ChIP-qPCR explored H3K27me3 enrichment at the *MIR203A* promoter (**K**), dual-luciferase reporter assay analyzed transcriptional activity of the *MIR203A* promoter (**L**) in different groups (n = 4). **M** qRT-PCR detected *MIR203A* and *SNAI2* levels (n = 4). **N** Co-IP detected the interaction between HOXB9 and EZH2 in different groups. **O** and **P** ChIP-qPCR explored H3K27me3 enrichment at the *MIR203A* promoter (**O**), dual-luciferase reporter assay analyzed transcriptional activity of the *MIR203A* promoter (**P**) in different groups (n = 4). **Q** qRT-PCR detected *MIR203A* and *SNAI2* levels in HCCLM3 cells with the indicated treatments (n = 4). Data are represented as the mean ± SD. ns, $p > 0.05$, $^{*}p < 0.05$, $^{**}p < 0.01$ and $^{***}p < 0.001$

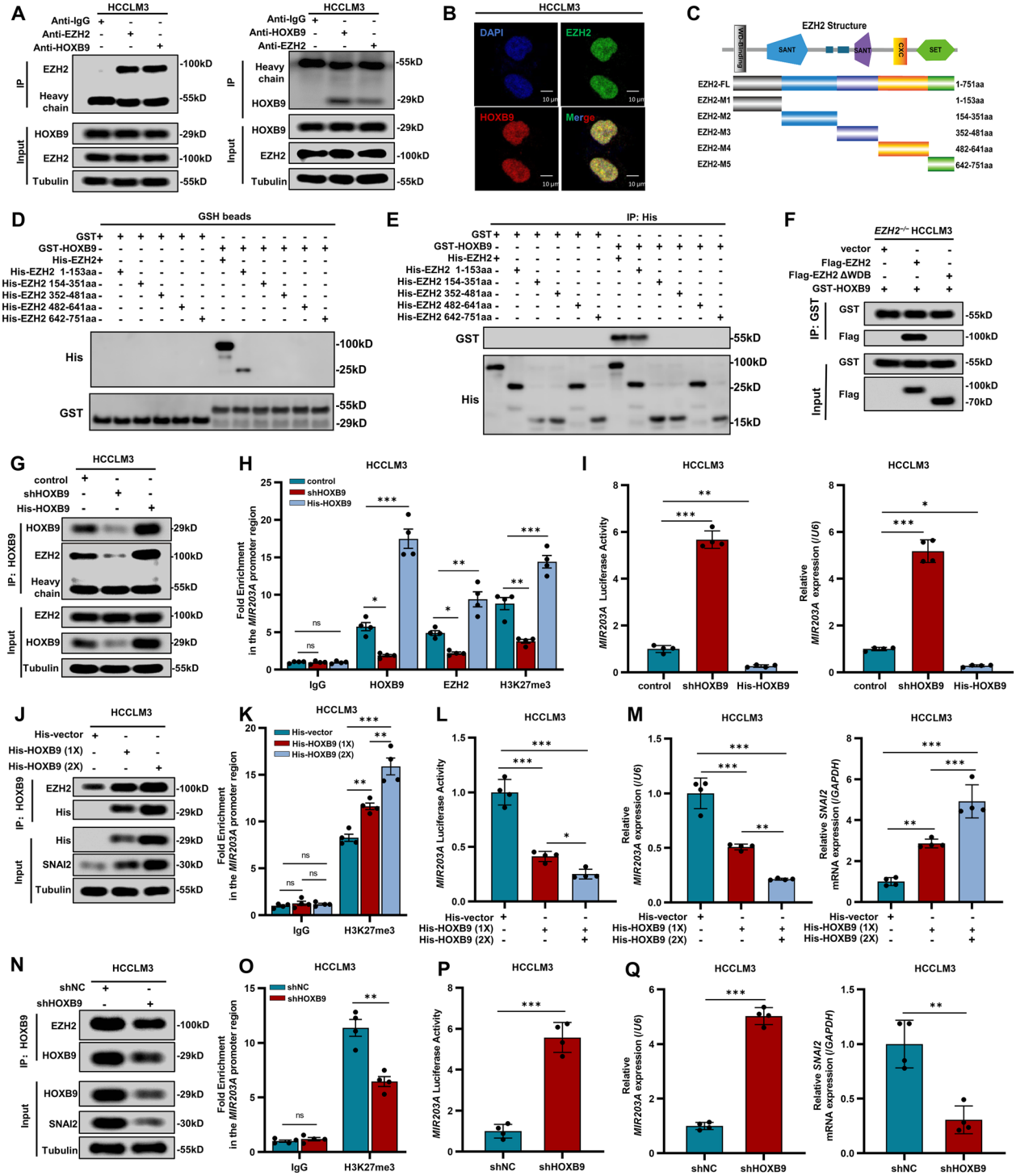

Fig. 6 (See legend on previous page.)

SNAI2 expression induced by HOXB9 overexpression, and the ISH results demonstrated that GSK126 treatment counteracted the reduction in *MIR203A* expression caused by HOXB9 overexpression (Fig. 7I, Fig. S8H). Together, our results indicated that GSK126 can attenuate the HOXB9-mediated enhancement of *MIR203A* silencing and subsequently decrease the expression of SNAI2 to inhibit the invasion and metastasis of HCC cells in vitro and in vivo.

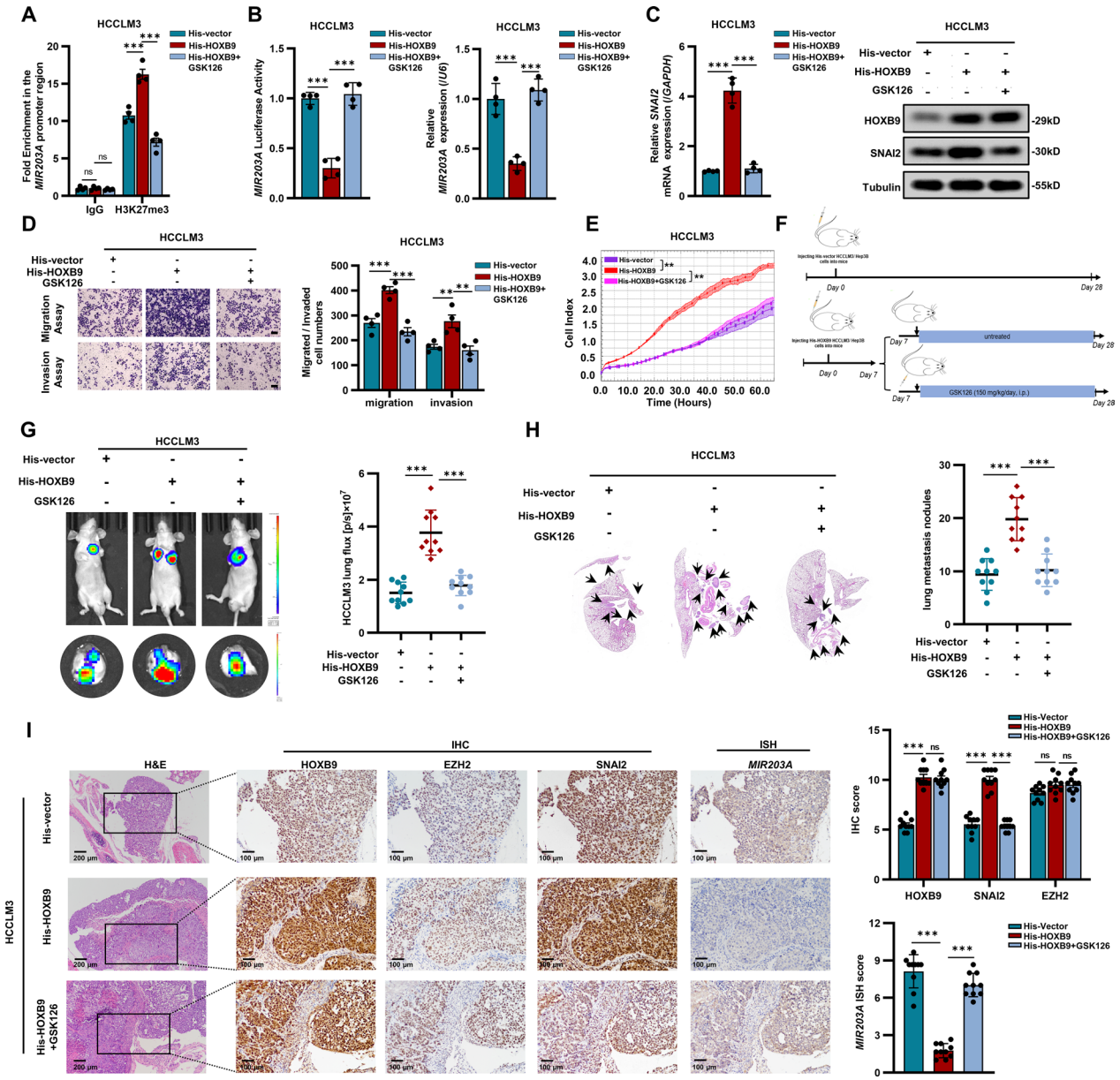

Fig. 7 Mitigating HOXB9-reduced *MIR203A* inhibits SNAI2-mediated invasion and metastasis of HCC cells. **A** ChIP-qPCR assay explored H3K27me3 enrichment at the *MIR203A* promoter in HCCLM3 cells with the indicated treatments (n = 4). **B** Dual-luciferase reporter assay and qRT-PCR detected transcriptional activity of the *MIR203A* promoter and *MIR203A* expression in HCCLM3 cells with the indicated treatments (n = 4). **C** qRT-PCR and western blot were used to detect the *SNAI2* mRNA and the protein expression of HOXB9 and SNAI2 in HCCLM3 cells with the indicated treatments (n = 4). **D** Transwell assays detected the migration and invasion of HCCLM3 cells with the indicated treatments (n = 4). Scale bars = 100 μm. **E** RTCA detected the invasion ability of HCCLM3 cells with the indicated treatments (n = 4). **F** Schematic diagram of lung metastasis of HCC cells in nude mice model and evaluating the effect of GSK126 in mice injecting His-HOXB9 HCCLM3/Hep3B cells. **G** and **H** Representative bioluminescent images and quantification analysis (**G**) of lung tumors in nude mice and H&E-stained images and quantification analysis (**H**) of metastatic nodules in the lungs (n = 10 mice per group). **I** IHC detected HOXB9, EZH2 and SNAI2 protein expression, and ISH detected *MIR203A* levels in the metastatic pulmonary tumors. Scale bars = 200 μm and 100 μm. Data are represented as the mean ± SD. ns, $p > 0.05$, $^{**}p < 0.01$ and $^{***}p < 0.001$

Discussion

Numerous studies have shown that HOXB9 plays an important role in promoting the invasion and metastasis of various tumors [15, 17, 38, 39]. However, the role of HOXB9 in promoting the invasion and metastasis of HCC cells remains largely unknown and requires further

exploration. In this study, we discovered a novel mechanism by which HOXB9 promotes invasion and metastasis of HCC cells by regulating the EZH2–MIR203A–SNAI2 axis (Fig. 8). Our results showed that HOXB9 can promote the invasion and metastasis of HCC cells by upregulating the expression of SNAI2. Further mechanistic studies revealed that HOXB9 can recruit EZH2 to the *MIR203A* promoter region, increase H3K27me3 in the *MIR203A* promoter region, inhibit *MIR203A* transcriptional activity and expression, upregulate SNAI2 expression in HCC cells. Finally, our in vitro and in vivo experimental results revealed that GSK126 attenuated the increases in the H3K27me3 level in the *MIR203A* promoter region induced by HOXB9 overexpression, promoted the transcriptional activity and expression of *MIR203A*, inhibited the expression of SNAI2, and thus suppressed the invasion and metastasis of HCC cells.

As a master transcription activator, HOXB9 mainly binds to the promoter regions of downstream oncogenes to increase their transcriptional activity and expression, thereby promoting tumor progression. For example, researches have indicated that HOXB9 can directly bind to the promoter regions of downstream oncogenes, such as the transcription factor E2F3 (*E2F3*), serine/arginine-rich splicing factor 3 (*SRSF3*), and microRNA 765 (*MIR765*), to upregulate their transcription activity and expression, thereby promoting the progression of various cancers [38, 40, 41]. However, whether and how HOXB9 can decrease the transcriptional activity of tumor suppressor genes to reduce their expression levels, thereby promoting tumor progression, has not yet been reported. Interestingly, our results confirmed that HOXB9 can decrease the transcriptional activity and expression of *MIR203A*, a tumor suppressor gene, by promoting H3K27me3 of its promoter, thereby promoting the invasion and metastasis of HCC cells. To our knowledge, this is the first study demonstrating that HOXB9 has the function of inhibiting the transcriptional activity and expression of tumor suppressor gene, and explain its underlying mechanism. This insight not only expands our understanding of the role of HOXB9 in cancer biology but also provide new perspectives for elucidating its function in tumorigenesis and progression.

EZH2, a methyltransferase, mainly promotes H3K27me3 in the promoter region of downstream tumor suppressor genes, which in turn silences their expression and consequently promotes the occurrence and development of various tumors [42–46]. However, studies

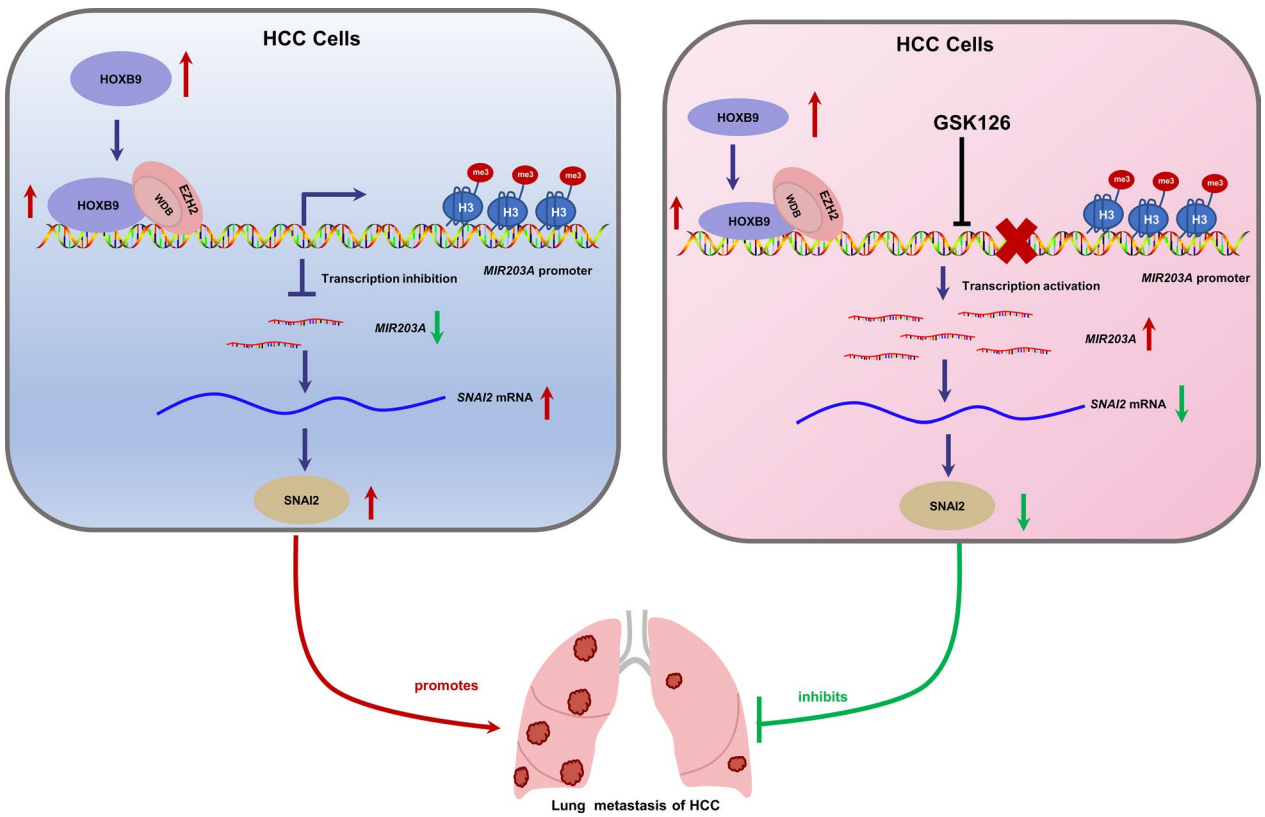

Fig. 8 The proposed model by which HOXB9 promotes invasion and metastasis of HCC cells via the EZH2-MIR203A-SNAI2 axis

have indicated that EZH2 itself cannot bind directly to the promoter regions of downstream target genes and requires other factors, such as transcription factors and noncoding RNAs, for its recruitment to the promoter regions of downstream genes to function as methyltransferases [47–50]. Thus, identifying new factors that recruit EZH2 to promote H3K27me3 in the downstream gene promoter region is crucial for understanding the role of EZH2 in tumorigenesis and development. Here, we discovered that HOXB9 can also recruit EZH2 to increase H3K27me3 in the *MIR203A* promoter region, thereby inhibiting the transcription and expression of *MIR203A* in HCC cells. In addition, EZH2 inhibitors have become a key strategy in clinical anti-tumor treatment, and identifying the anti-tumor targets of EZH2 inhibitors has emerged as a major research focus [43, 51–55]. Interestingly, we have identified a new target of GSK126, an EZH2 inhibitor, which can activate the expression of the tumor suppressor gene *MIR203A*, and subsequently reducing the invasion and metastasis of HCC cells. This funding provides a new theoretical basis for the clinical application of EZH2 inhibitors in anti-tumor therapy.

However, the present study also has several limitations that warrant consideration. First, the role of the HOXB9–EZH2–MIR203A–SNAI2 axis has only been validated in cellular and animal models, with a lack of clinical evidence, and therefore, further clinical studies are required to confirm this axis significance. In addition, our research focused only on exploring the impact of HOXB9-mediated epigenetic silencing of the tumor suppressor *MIR203A* in HCC cells. Further exploration is needed to investigate the role of HOXB9-mediated epigenetic silencing of other tumor suppressor genes in different tumor cells.

Conclusion

In conclusion, we decipher the role of the HOXB9–EZH2–MIR203A–SNAI2 axis in the invasion and metastasis of HCC cells and unveil a novel mechanism of HOXB9 promoting invasion and metastasis in HCC cells. This finding provides a new theoretical basis for understanding the mechanisms of invasion and metastasis in HCC cells and for developing treatment strategies.

Abbreviations

ChIP-seq	Chromatin immunoprecipitation, followed by sequencing
ChIRP-seq	The chromatin isolation by RNA purification sequencing
Co-IP	Co-immunoprecipitation
DZNeP	3-Deazaneplanocin A
EZH2	Enhancer of zeste homolog 2
GSK126	GSK2816126A
GST pull-down	Glutathione S-transferase-pull-down
HOXB9	Homeobox B9
HCC	Hepatocellular carcinoma
H3K27me3	Histone H3 lysine 27 methylation
IVIS	In vivo imaging system
IHC	Immunohistochemistry
ISH	In-situ hybridization
miRNAs	Micro-RNAs
miRNA-seq	MiRNA sequencing
MIR203A	MicroRNA-203a
qRT-PCR	Quantitative reverse transcription polymerase chain reaction
RNA-seq	RNA sequencing
RTCA	Real-Time Cell Kinetic Analyzer
SNAI2	Snail family transcriptional repressor 2

Supplementary Information

The online version contains supplementary material available at https://doi.org/10.1186/s12967-024-05690-x.

Supplementary Material 1.

Acknowledgements

Not applicable.

Author contributions

D.D. Zhang carried out major western blotting, bioinformatics, cellular, and animal studies and wrote the original draft. Y.M. Qiu carried out western blotting, cellular and animal studies. W.M. Zhang and D.N. Du were responsible for immunohistochemistry and in-situ hybridization. Y. Liu performed some in vivo animal experiments. J.J. Li and L.P. Liu performed RTCA assays. X.Z. Yu, Z.H. Chen and M. Ye conducted in vitro transwell assays. W. Wang and Z.J. Li conducted immunofluorescence assays. J.H. Shao was responsible for supervising the project, providing funding support, writing the original draft, writing review & editing. All authors have read and approved the final manuscript.

Funding

This work was supported by the National Natural Science Foundation of China (81560475, 81773126, 82160486), the Project of Jiangxi Provincial Department of Science and Technology (20223BCG74008).

Data availability

The data supporting the findings reported in this article are available upon request from the corresponding author upon reasonable request.

Declarations

Ethics approval and consent to participate

All animal experiments were approved by the Animal Use Ethical Committee of Nanchang University. Animal studies were performed in accordance with the Guide for the Care and Use of Laboratory Animals Consent for publication.

Competing interests

The authors have declared that no competing interest exists.

Author details

[1]Department of General Surgery, Second Affiliated Hospital of Nanchang University, Nanchang 330000, China. [2]Jiangxi Province Key Laboratory of Molecular Medicine, Second Affiliated Hospital of Nanchang University, Nanchang 330000, China. [3]Liver Cancer Institute, Nanchang University, Nanchang 330000, China. [4]Jiangxi Province Clinical Research Center of General Surgery, Second Affiliated Hospital of Nanchang University, Nanchang 330000, China. [5]Department of Cardiovascular Medicine, Second Affiliated Hospital of Nanchang University Nanchang, Nanchang 330000, China. [6]The MOE Basic Research and Innovation Center for the Targeted Therapeutics of Solid Tumors, Nanchang University, Nanchang, China.

Received: 8 July 2024 Accepted: 17 September 2024
Published online: 10 October 2024

References

1. Sung H, Ferlay J, Siegel RL, Laversanne M, Soerjomataram I, Jemal A, Bray F. Global cancer statistics 2020: GLOBOCAN estimates of incidence and mortality worldwide for 36 cancers in 185 countries. CA Cancer J Clin. 2021;71(3):5146.
2. Yang JD, Hainaut P, Gores GJ, Amadou A, Plymoth A, Roberts LR. A global view of hepatocellular carcinoma: trends, risk, prevention and management. Nat Rev Gastroenterol Hepatol. 2019;16(10):589–604.
3. Llovet JM, Kelley RK, Villanueva A, Singal AG, Pikarsky E, Roayaie S, Lencioni R, Koike K, Zucman-Rossi J, Finn RS. Hepatocellular carcinoma. Nat Rev Dis Primers. 2021;7(1):6.
4. Lewis EB. A gene complex controlling segmentation in Drosophila. Nature. 1978;276(5688):565–70.
5. Malicki J, Bogarad LD, Martin MM, Ruddle FH, McGinnis W. Functional analysis of the mouse homeobox gene HoxB9 in Drosophila development. Mech Dev. 1993;42(3):139–50.
6. McGinnis W, Krumlauf R. Homeobox genes and axial patterning. Cell. 1992;68(2):283–302.
7. Chen F, Capecchi MR. Paralogous mouse Hox genes, Hoxa9, Hoxb9, and Hoxd9, function together to control development of the mammary gland in response to pregnancy. Proc Natl Acad Sci U S A. 1999;96(2):541–6.
8. Shrestha B, Ansari KI, Bhan A, Kasiri S, Hussain I, Mandal SS. Homeodomain-containing protein HOXB9 regulates expression of growth and angiogenic factors, facilitates tumor growth in vitro and is overexpressed in breast cancer tissue. FEBS J. 2012;279(19):3715–26.
9. Hayashida T, Takahashi F, Chiba N, Brachtel E, Takahashi M, Godin-Heymann N, Gross KW, Vivanco M, Wijendran V, Shioda T, et al. HOXB9, a gene overexpressed in breast cancer, promotes tumorigenicity and lung metastasis. Proc Natl Acad Sci U S A. 2010;107(3):1100–5.
10. Martinou E, Moller-Levet C, Karamanis D, Bagwan I, Angelidi AM. HOXB9 overexpression promotes colorectal cancer progression and is associated with worse survival in liver resection patients for colorectal liver metastases. Int J Mol Sci. 2022;23(4):2281.
11. Huang K, Yuan R, Wang K, Hu J, Huang Z, Yan C, Shen W, Shao J. Overexpression of HOXB9 promotes metastasis and indicates poor prognosis in colon cancer. Chin J Cancer Res. 2014;26(1):72–80.
12. Seki H, Hayashida T, Jinno H, Hirose S, Sakata M, Takahashi M, Maheswaran S, Mukai M, Kitagawa Y. HOXB9 expression promoting tumor cell proliferation and angiogenesis is associated with clinical outcomes in breast cancer patients. Ann Surg Oncol. 2012;19(6):1831–40.
13. Zhan J, Wang P, Niu M, Wang Y, Zhu X, Guo Y, Zhang H. High expression of transcriptional factor HoxB9 predicts poor prognosis in patients with lung adenocarcinoma. Histopathology. 2015;66(7):955–65.
14. Li F, Dong L, Xing R, Wang L, Luan F, Yao C, Ji X, Bai L. Homeobox B9 is overexpressed in hepatocellular carcinomas and promotes tumor cell proliferation both in vitro and in vivo. Biochem Biophys Res Commun. 2014;444(2):241–7.
15. Bai L, Ge P, Zhang Y, Song Y, Xing R, Zhou D. Homeobox B9 promotes the progression of hepatocellular carcinoma via TGF-beta1/Smad and ERK1/2 signaling pathways. Biomed Res Int. 2022;2022:1080315.
16. Chiba N, Ozawa Y, Hikita K, Okihara M, Sano T, Tomita K, Takano K, Kawachi S. Increased expression of HOXB9 in hepatocellular carcinoma predicts poor overall survival but a beneficial response to sorafenib. Oncol Rep. 2017;37(4):2270–6.
17. Yuan R, Wang K, Hu J, Yan C, Li M, Yu X, Liu X, Lei J, Guo W, Wu L, et al. Ubiquitin-like protein FAT10 promotes the invasion and metastasis of hepatocellular carcinoma by modifying beta-catenin degradation. Cancer Res. 2014;74(18):5287–300.
18. Zhou W, Gross KM, Kuperwasser C. Molecular regulation of Snai2 in development and disease. J Cell Sci. 2019;132(23):jcs235127.
19. Shioiri M, Shida T, Koda K, Oda K, Seike K, Nishimura M, Takano S, Miyazaki M. Slug expression is an independent prognostic parameter for poor survival in colorectal carcinoma patients. Br J Cancer. 2006;94(12):1816–22.
20. Shih JY, Tsai MF, Chang TH, Chang YL, Yuan A, Yu CJ, Lin SB, Liou GY, Lee ML, Chen JJ, et al. Transcription repressor slug promotes carcinoma invasion and predicts outcome of patients with lung adenocarcinoma. Clin Cancer Res. 2005;11(22):8070–8.
21. Jin Y, Chen L, Li L, Huang G, Huang H, Tang C. SNAI2 promotes the development of ovarian cancer through regulating ferroptosis. Bioengineered. 2022;13(3):6451–63.
22. Fan H, Wang X, Li W, Shen M, Wei Y, Zheng H, Kang Y. ASB13 inhibits breast cancer metastasis through promoting SNAI2 degradation and relieving its transcriptional repression of YAP. Genes Dev. 2020;34(19–20):1359–72.
23. Wang W, Hind T, Lam BWS, Herr DR. Sphingosine 1-phosphate signaling induces SNAI2 expression to promote cell invasion in breast cancer cells. FASEB J. 2019;33(6):7180–91.
24. Sun Y, Song GD, Sun N, Chen JQ, Yang SS. Slug overexpression induces stemness and promotes hepatocellular carcinoma cell invasion and metastasis. Oncol Lett. 2014;7(6):1936–40.
25. Wang Z, Zhao Z, Yang Y, Luo M, Zhang M, Wang X, Liu L, Hou N, Guo Q, Song T, et al. MiR-99b-5p and miR-203a-3p function as tumor suppressors by targeting IGF-1R in gastric cancer. Sci Rep. 2018;8(1):10119.
26. Jiang N, Jiang X, Chen Z, Song X, Wu L, Zong D, Song D, Yin L, Wang D, Chen C, et al. MiR-203a-3p suppresses cell proliferation and metastasis through inhibiting LASP1 in nasopharyngeal carcinoma. J Exp Clin Cancer Res. 2017;36(1):138.
27. Diao Y, Guo X, Jiang L, Wang G, Zhang C, Wan J, Jin Y, Wu Z. miR-203, a tumor suppressor frequently down-regulated by promoter hypermethylation in rhabdomyosarcoma. J Biol Chem. 2014;289(1):529–39.
28. Furuta M, Kozaki KI, Tanaka S, Arii S, Imoto I, Inazawa J. miR-124 and miR-203 are epigenetically silenced tumor-suppressive microRNAs in hepatocellular carcinoma. Carcinogenesis. 2010;31(5):766–76.
29. Xiao JN, Yan TH, Yu RM, Gao Y, Zeng WL, Lu SW, Que HX, Liu ZP, Jiang JH. Long non-coding RNA UCA1 regulates the expression of Snail2 by miR-203 to promote hepatocellular carcinoma progression. J Cancer Res Clin Oncol. 2017;143(6):981–90.
30. Ma J, Zhang J, Weng YC, Wang JC. EZH2-mediated microRNA-139-5p regulates epithelial-mesenchymal transition and lymph node metastasis of pancreatic cancer. Mol Cells. 2018;41(9):868–80.
31. Wang Q, Liu S, Wang H, Liu L, Zhang S, Ming Y, Zhao Y, Cheng K. Silencing long noncoding RNA NEAT1 alleviates acute liver failure via the EZH2-mediated microRNA-139/PUMA axis. Aging (Albany NY). 2021;13(9):12537–51.
32. Ning X, Shi Z, Liu X, Zhang A, Han L, Jiang K, Kang C, Zhang Q. DNMT1 and EZH2 mediated methylation silences the microRNA-200b/a/429 gene and promotes tumor progression. Cancer Lett. 2015;359(2):198–205.
33. Kotipalli A, Banerjee R, Kasibhatla SM, Joshi R. Analysis of H3K4me3-ChIP-Seq and RNA-Seq data to understand the putative role of miRNAs and their target genes in breast cancer cell lines. Genomics Inform. 2021;19(2):e17.
34. Li J, Sha Z, Zhu X, Xu W, Yuan W, Yang T, Jin B, Yan Y, Chen R, Wang S, et al. Targeting miR-30d reverses pathological cardiac hypertrophy. EBioMedicine. 2022;81: 104108.
35. Cisneros-Soberanis F, Andonegui MA, Herrera LA. miR-125b-1 is repressed by histone modifications in breast cancer cell lines. Springerplus. 2016;5(1):959.
36. Wang K, Jiang X, Jiang Y, Liu J, Du Y, Zhang Z, Li Y, Zhao X, Li J, Zhang R. EZH2-H3K27me3-mediated silencing of mir-139-5p inhibits cellular senescence in hepatocellular carcinoma by activating TOP2A. J Exp Clin Cancer Res. 2023;42(1):320.
37. Yang Y, Zhou L, Lu L, Wang L, Li X, Jiang P, Chan LK, Zhang T, Yu J, Kwong J, et al. A novel miR-193a-5p-YY1-APC regulatory axis in human endometrioid endometrial adenocarcinoma. Oncogene. 2013;32(29):3432–42.
38. Wan J, Liu H, Feng Q, Liu J, Ming L. HOXB9 promotes endometrial cancer progression by targeting E2F3. Cell Death Dis. 2018;9(5):509.
39. Sun C, Deng H, Li Q, Wang P, Chen Y, Sun Y, Han C. HOXB9 promotes laryngeal squamous cell carcinoma progression by upregulating MMP12. Funct Integr Genomics. 2024;24(3):78.
40. Yuan L, Cheng F, Wu Z, Li X, Shen W. Homeobox B9 promotes colon cancer progression by targeting SRSF3. Dig Dis Sci. 2023;68(8):3324–40.
41. Lin J, Zhang D, Fan Y, Chao Y, Chang J, Li N, Han L, Han C. Regulation of cancer stem cell self-renewal by HOXB9 antagonizes endoplasmic reticulum stress-induced melanoma cell apoptosis via the miR-765-FOXA2 axis. J Invest Dermatol. 2018;138(7):1609–19.
42. Li N, Geng F, Liang SM, Qin X. USP7 inhibits TIMP2 by up-regulating the expression of EZH2 to activate the NF-kappaB/PD-L1 axis to promote the development of cervical cancer. Cell Signal. 2022;96: 110351.
43. Kim KH, Roberts CW. Targeting EZH2 in cancer. Nat Med. 2016;22(2):128–34.

44. Chen Z, Tang W, Zhou Y, He Z. The role of LINC01419 in regulating the cell stemness in lung adenocarcinoma through recruiting EZH2 and regulating FBP1 expression. Biol Direct. 2022;17(1):23.
45. Li Y, Li D, Zhao M, Huang S, Zhang Q, Lin H, Wang W, Li K, Li Z, Huang W, et al. Long noncoding RNA SNHG6 regulates p21 expression via activation of the JNK pathway and regulation of EZH2 in gastric cancer cells. Life Sci. 2018;208:295–304.
46. Yin D, Lu X, Su J, He X, De W, Yang J, Li W, Han L, Zhang E. Long noncoding RNA AFAP1-AS1 predicts a poor prognosis and regulates non-small cell lung cancer cell proliferation by epigenetically repressing p21 expression. Mol Cancer. 2018;17(1):92.
47. Surface LE, Thornton SR, Boyer LA. Polycomb group proteins set the stage for early lineage commitment. Cell Stem Cell. 2010;7(3):288–98.
48. Cao R, Zhang Y. The functions of E(Z)/EZH2-mediated methylation of lysine 27 in histone H3. Curr Opin Genet Dev. 2004;14(2):155–64.
49. Pu FF, Shi DY, Chen T, Liu YX, Zhong BL, Zhang ZC, Liu WJ, Wu Q, Wang BC, Shao ZW, et al. SP1-induced long non-coding RNA SNHG6 facilitates the carcinogenesis of chondrosarcoma through inhibiting KLF6 by recruiting EZH2. Cell Death Dis. 2021;12(1):59.
50. Chen H, Hou G, Yang J, Chen W, Guo L, Mao Q, Ge J, Zhang X. SOX9-activated PXN-AS1 promotes the tumorigenesis of glioblastoma by EZH2-mediated methylation of DKK1. J Cell Mol Med. 2020;24(11):6070–82.
51. Duan R, Du W, Guo W. EZH2: a novel target for cancer treatment. J Hematol Oncol. 2020;13(1):104.
52. Huang X, Yan J, Zhang M, Wang Y, Chen Y, Fu X, Wei R, Zheng XL, Liu Z, Zhang X, et al. Targeting epigenetic crosstalk as a therapeutic strategy for EZH2-aberrant solid tumors. Cell. 2018;175(1):186–99.
53. Yu J, Yang K, Zheng J, Zhao P, Xia J, Sun X, Zhao W. Activation of FXR and inhibition of EZH2 synergistically inhibit colorectal cancer through cooperatively accelerating FXR nuclear location and upregulating CDX2 expression. Cell Death Dis. 2022;13(4):388.
54. Zong X, Wang W, Ozes A, Fang F, Sandusky GE, Nephew KP. EZH2-mediated downregulation of the tumor suppressor DAB2IP maintains ovarian cancer stem cells. Cancer Res. 2020;80(20):4371–85.
55. Chen W, Tang D, Tang D, Dai Y. Epigenetic silencing of ZIC4 contributes to cancer progression in hepatocellular carcinoma. Cell Death Dis. 2020;11(10):906.

Publisher's Note